Stimulated dynamic light scattering

H. Z. Wang, X. G. Zheng, W. D. Mao, Z. X. Yu, and Z. L. Gao
Institute for Laser and Spectroscopy, Zhongshan University, Guangzhou 510275, China
(Received 18 October 1994)

Stimulated dynamic light scattering (SDLS) in CS_2 is studied by time-resolved pump-density-dependent experiments in this paper. It is found that SDLS consists of two main contributions, one of which dominates at the rise time of the pump pulse, and the other around the peak of the high-density pump pulse. The former is related to molecular orientation, damped intermolecular vibration, and molecular trnaslation, while the latter is related to intermolecular interactions. Our experimental results demonstrate that the SDLS due to dipole interaction has a higher pump-power-density dependence than stimulated Raman scattering and SDLS due to molecular motions. The present experimental results also demonstrate that the threshold of SDLS due to molecular motions depends on the pump-pulse duration. SDLS can be greatly enhanced by extending the interaction length in a liquid-core waveguide. In our experiments, the efficiency of SDLS is nearly 100% and the frequency shift of SDLS covers hundreds of wave numbers in CS_2 bulk liquid and 5000 cm^{-1} in a CS_2 liquid-core waveguide.

PACS number(s): 42.65.−k, 33.20.Fb, 34.20.Gj, 78.30.Cp

I. INTRODUCTION

Light scattering is the result of the interaction between light and material excitation. Dynamic light scattering of molecules is related to intermolecular motion and interaction; it is, therefore, a rich source of dynamical and structural information which is not always available by other techniques. Applications of dynamic light scattering to problems in physics, chemistry, biology, medicine, and fluid mechanics have proliferated [1]. Spontaneous dynamic light scattering of molecules in liquid consists of two primary components: (1) scattering due to intermolecular motions, including molecular orientation, damped intermolecular vibration, and molecular translational movement; (2) scattering due to intermolecular interaction of dipole-induced dipoles, collision induced, and so on [1–10]. It has been demonstrated theoretically and experimentally that the frequency shift of scattering due to molecular orientation is less than 20 cm^{-1}, and the frequency shift of scattering due to damped intermolecular vibration, molecular translational movement, dipole-induced dipoles, and the collision-induced effect has been found in the range from 20 to more than 100 cm^{-1} [1–10].

Dynamic light scattering is also called depolarized light scattering. Dynamic light scattering of the excitation line is called Rayleigh-wing scattering, and that of the Raman line is called Raman-wing scattering. When the pump density is high enough, stimulated Rayleigh-wing scattering can be observed [11–14]. The spectral line shape and broadening behavior of stimulated Rayleigh-wing scattering is quite different from those of spontaneous Rayleigh-wing scattering. For example, the spontaneous Rayleigh-wing scattering of liquid has a nearly symmetric spectral distribution [1–10]. However, the previously reported experimental and theoretical results of stimulated Rayleigh-wing scattering show only an asymmetric Stokes spectral distribution [11–14].

Recently, a large Stokes broadening stimulated dynamic light scattering (SDLS), excited by an ultashort pulse laser, has been investigated by several groups [15–20]. In the previous reports, an effective broadband SDLS has been obtained at a lower pump density as a result of the interaction length extending in a waveguide [15–19]. The broadband SDLS is applicable to transient spectroscopy [15,19], laser pulse compression [16], and the studies of molecular dynamics. However, some important subjects, such as pump-density-dependent temporal behavior of SDLS and competition between SDLS and the other third-order nonlinear effects, have not been studied. Especially, it has not been reported which intermolecular motions and interactions is related to SDLS, and the corresponding transient behaviors have not been investigated.

SDLS of molecules in liquid, similar to spontaneous dynamic light scattering, consists of two primary contributions. The first contribution is related to intermolecular motion, including molecular orientation [14], damped intermolecular vibration [21], and molecular translational movement. Because the duration of the nanosecond (ns) pump laser pulse in this work is much longer than the duration that the molecular orientational distribution tends to equilibrium with the light field against thermal randomization and against the interaction force between molecules in high alignment, the degree of molecular alignment will increase with the transient pump power at the rise time of the pump pulse. Also, the other molecular motions are accompanied by molecular orientation. Therefore, the first contribution is only effective at the rise time of the nanosecond pump pulse. The nonlinear susceptibility and gain under the condition of equilibrium has been theoretically studied [14]. However, with picosecond (ps) pulse laser pumping, the rise time of the pump pulse is shorter than the time that the molecular orientational distribution tends to equilibrium with the light field, i.e., under the condition of nonequilibrium.

The second contribution is not only related to the dipole-induced dipoles and collision-induced effect, which is similar to that in spontaneous dynamic light scattering, but is also related to the interaction between light-induced dipoles for dense fluids with high third-order susceptibility and high polarizability such as CS_2 in a self-focus filament.

In this paper, systematical experimental investigations reveal the pump-density-dependent temporal and spectral behaviors of each component of SDLS.

II. EXPERIMENTAL APPARATUS

The experimental arrangement is shown in Fig. 1. The experiments are performed with a frequency-doubled passively mode-locked Nd:YAG (where YAG denotes yttrium aluminum garnet) laser and a frequency-doubled saturable absorber Q-switch Nd:YAG laser as pump source. The pulse durations of the passively mode-locked Nd:YAG laser and the Q-switch Nd:YAG laser are 40 ps and 6 ns, respectively, which are longer than the time for self-focus filament forming. The scattering is detected by a single pulse sweep streak camera (Hamamatsu Model C1587, 2 ps time resolution) connected to a polychromator, thus the spectral and temporal characteristics can be recorded simultaneously. F_1 in Fig. 1 is a HA30 color filter for cutting off 1.06 μm fundamental wave. F_2 and F_3 are neutral filters. In this work, scattering both in a CS_2 bulk liquid and in a CS_2 liquid-core waveguide are studied. A glass capillary, 1.0 m long and 0.5 mm internal diameter, is employed as the waveguide. The pump laser is coupled into waveguide with a lens of 75 cm focal length. A lens of 5 cm focal length is employed to focus the laser beam into the cell for high density and short interaction length. Different from experimental arrangements for the study of self-phase-modulation, there is not any color filter for cutting off pump light between the cell and the streak camera.

III. EXPERIMENTAL RESULTS AND DISCUSSIONS

A. Temporal and spectral behavior of SDLS in a liquid-core waveguide

Figures 2 and 3 show the temporal behavior of SDLS and stimulated Raman scattering in a CS_2 liquid-core waveguide excited by a frequency-doubled Q-switch Nd:YAG laser and a mode-locked Nd:YAG laser, respectively. In both cases, the excitation average power density is 0.2 GW/cm^2. Here and thereinafter the excitation average power density is a spatial average in a laser beam cross section. At the start of the pump pulse, SDLS appears later than the stimulated Raman scattering in Fig. 2, and earlier than stimulated Raman scattering in Fig. 3. It means that the threshold of SDLS decreases with the shortening of the pump-pulse duration.

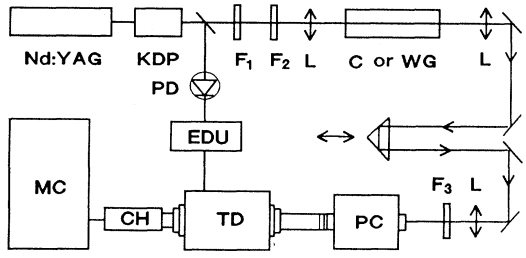

FIG. 1. Schematic diagram of experimental apparatus. Nd:YAG—mode locked or Q-switch Nd:YAG laser, KDP—second harmonic crystal, C or WG—cell or waveguide, PD—photodiode, F—filter, L—lens, EDU—electric delay unit, PC—polychromator, TD—time dispersion unit, CH—camera head, MC—microcomputer.

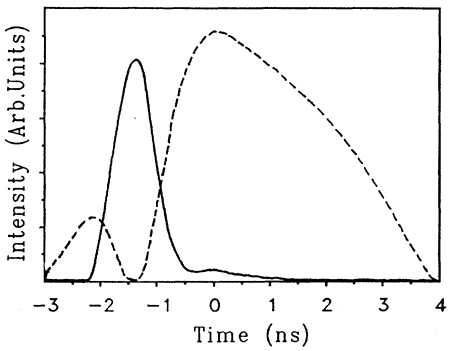

FIG. 2. Temporal behaviors of SDLS (solid line) and stimulated Raman scattering (dashed line) in a CS_2 liquid-core waveguide excited by a frequency-doubled Q-switch Nd:YAG laser of 0.2 GW/cm^2 average power density.

The solid line in Fig. 2 shows the temporal behavior of SDLS excited by a nanosecond pulse laser of 0.2 GW/cm^2 average power density. It is clear that the solid line is composed of two components. The first component dominates at the rise time of the pump pulse, with a scattering pulse duration shorter than the rise time of the pump pulse. It is stimulated scattering due to intermolecular motion. The second component is very weak at 0.2 GW/cm^2 average pump-power density. The peak of the second component is correlated to the peak of the pump pulse. The pump-pulse peak is selected as the origin of time axis in Fig. 2, although the waveform of the

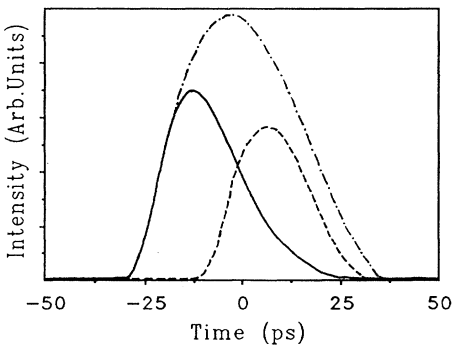

FIG. 3. Temporal behaviors of SDLS (solid line) and stimulated Raman scattering (dashed line) in a CS_2 liquid-core waveguide excited by a frequency-doubled mode-locked Nd:YAG laser of 0.2 GW/cm^2 average power density (dotted and dashed line: the pump pulse).

pump pulse was not recorded perfectly because the pump-pulse duration is longer than the sweep time range of our streak camera.

In Fig. 3, SDLS is effective at both the start and the rise time of the pump pulse. The scattering at the peak and the fall time of the pump pulse also mainly relates to molecular orientation as a result of a nonequilibrium condition with this low-density picosecond pulse pumping. This will be more clear in Sec. III B.

Figure 4 shows the temporal behavior of SDLS and stimulated Raman scattering in a CS_2 liquid-core waveguide excited by a picosecond pump laser of 10 GW/cm^2 average power density. In Fig. 4, SDLS is dominant, and stimulated Raman scattering only appears at the tail of the pump pulse.

Figure 5 shows the broadband SDLS spectrum in a waveguide excited by a picosecond pulse laser of 3 GW/cm^2 average power density. In Fig. 5, the broadband SDLS of a laser line and Raman lines connect with each other to form a super broadband covering 1000 wave numbers. Figure 6 shows the broadband SDLS spectrum in a waveguide excited by a picosecond pulse laser of 10 GW/cm^2 average power density. The broadening of nearly 3000 wave numbers in Fig. 6 is no longer the connection of a broadening pump line and a Raman line. It is directly shifted from the pump light. The three-dimensional spectra show clearly that the maximal broadening appears near the peak of the high-density pump pulse, and very weak broadening stimulated Raman scattering only appears at the tail of high-density pump pulse.

Furthermore, SDLS covers more than 5000 cm^{-1} at 20 GW/cm^2 average pump-power density. In the side view of the waveguide, the color of the waveguide changes from green at the input end to yellow, and to red, finally to dark red at the output end, at this high pump density. In the meantime, it has been verified by our experiment that the output light from the waveguide of 20 cm length has been depolarized. Therefore, the color changing in the latter 80 cm of the waveguide mainly results from the dipoles interaction. Moreover, the different color in different parts of the waveguide also implies that the

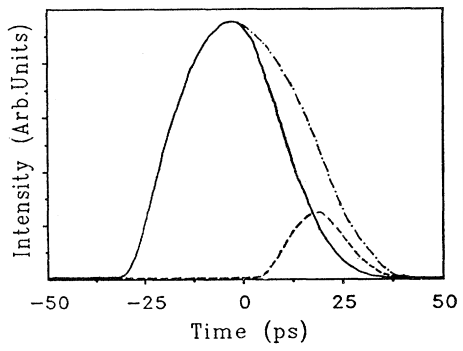

FIG. 4. Temporal behaviors of SDLS (solid line) and stimulated Raman scattering (dashed line) in a CS_2 liquid-core waveguide excited by a frequency-doubled mode-locked Nd:YAG laser of 10 GW/cm^2 average power density (dotted and dashed line: the pump pulse).

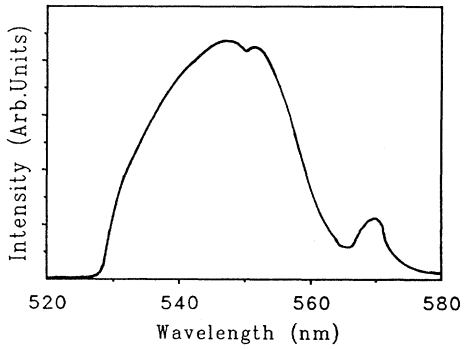

FIG. 5. Spectrum of SDLS in a CS_2 liquid-core waveguide excited by a frequency-doubled mode-locked Nd:YAG laser of 3 GW/cm^2 average power density.

SDLS light from the first part of the waveguide plays the pump light for the second part of the waveguide.

Summing up the experimental results above, at low-density picosecond pulse laser pumping, SDLS due to molecular motion dominates at the rise time of the pump pulse, stimulated Raman scattering dominates at the fall time of the pump pulse. Then, at high pump density, SDLS is dominant, and the maximal spectral broadening appears near the peak of the pump pulse; stimulated Raman scattering only appears at the tail of the pump pulse.

B. SDLS at high pump density in a CS_2 bulk cell

Surprisingly, only at the average pump-power density in the range from 0.1 MW/cm^2 to 1 GM/cm^2, the efficiency of SDLS is near 100% at the rise time of the picosecond pump pulse, with a Stokes shift of less than 20 cm^{-1}. A gradually weakened SDLS appears at the fall time of the pump pulse. Figure 7 shows the spectra of the output light at average pump-power density of 0.1 GW/cm^2.

At the average pump-power density in the range from 1 GW/cm^2 to 10 GW/cm^2, not only an effective Stokes shift of less than 20 cm^{-1} but also a weak Stokes shift in a range from 20 to more than 100 cm^{-1} appears at the duration from the rise time to the peak of the pump pulse, as shown in Fig. 8.

The effective Stokes shift of less than 20 cm^{-1} at the

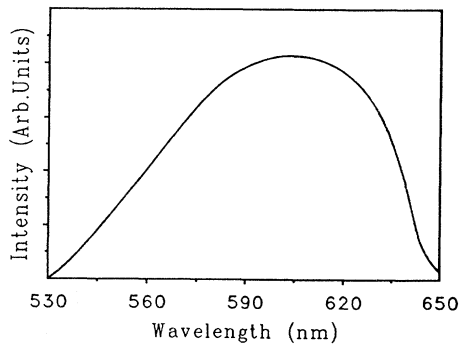

FIG. 6. Spectrum of SDLS in a CS_2 liquid-core waveguide excited by a frequency-doubled mode-locked Nd:YAG laser of 10 GW/cm^2 average power density.

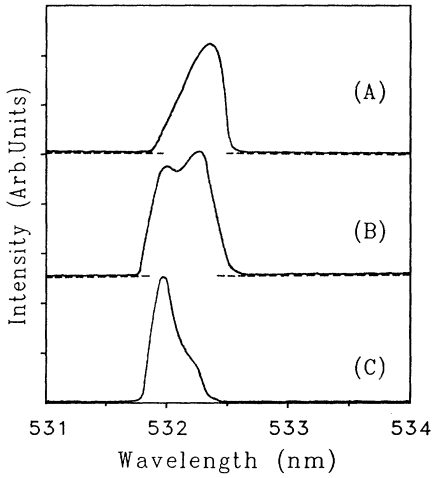

FIG. 7. Spectra of SDLS in a CS_2 bulk liquid cell excited by a frequency-doubled mode-locked Nd:YAG laser of 0.1 GW/cm^2 average power density: curve *A*, the rise time of the pump pulse; curve *B*, the peak of the pump pulse; curve *C*, the fall time of the pump pulse.

rise time of the pump pulse is consistent with the scattering due to molecular orientation [1–14], and the scattering at the peak and fall time of low pump-density pulse results from a nonequilibrium condition. The reported studies of SDLS in a waveguide [15–19] are mainly in this range of pump density, therefore the broadening in these studies mainly results from molecular orientation. Then, the weak Stokes shift in the range from 20 to more than 100 cm^{-1} in Fig. 8 relates to damped molecular vibration and molecular translational movement.

When the pump density further increases, the broadening increases with the pump density, as shown in Fig. 9. Different from that at low-pump density, the largest spectral broadening occurs near the peak of the pump pulse instead of the middle of the rise time when the average pump-power density is larger than 20 GW/cm^2, as shown in Fig. 10. This is because of the large interaction energy of dense-induced dipoles due to high-pump-power density. Curves *A*, *B*, *C*, *D*, and *E* in Fig. 10 are spectra detected at the peak, the rise time, the fall time, the start, and the tail of the pump pulse, respectively, at average pump-power density of 160 GW/cm^2. The spectral broadening of curve *B* in Fig. 10 is larger than that of curve *C*, and similarly the spectral broadening of curve *D* is much larger than that of curve *E*. This is due to effective intermolecular motion scattering at the start and the rise time of the pump pulse.

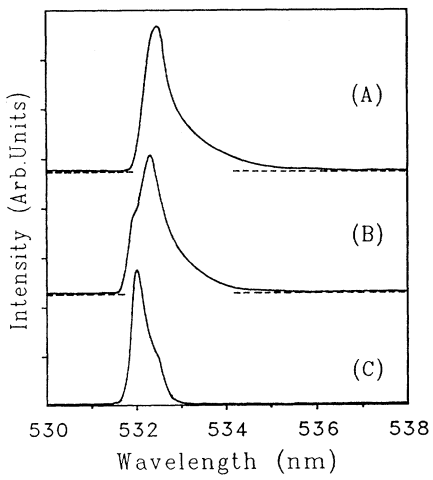

FIG. 8. Spectra of SDLS in a CS_2 bulk liquid cell excited by a frequency-doubled mode-locked Nd:YAG laser of 5 GW/cm^2 average power density: curve *A*, the rise time of the pump pulse; curve *B*, the peak of the pump pulse; curve *C*, the tail of the pump pulse.

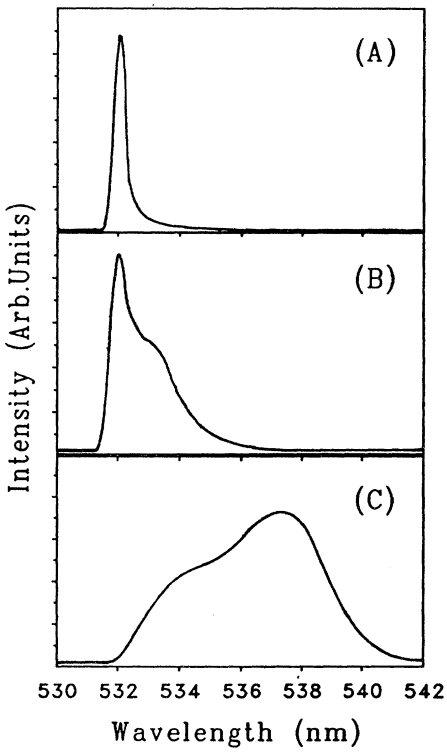

FIG. 9. Spectra of SDLS in a CS_2 bulk liquid cell excited by a frequency-doubled mode-locked Nd:YAG laser at average power density of (a) 3 GW/cm^2, (b) 30 GW/cm^2, and (c) 160 GW/cm^2.

Figure 10 shows a major differentiation between SDLS and self-phase modulation. There is a minimal spectral broadening of self-phase modulation at the peak of the pump pulse [14]. On the contrary, there is a maximal spectral broadening of SDLS at the peak of the high-density pump pulse.

To study the competition between SDLS and self-phase modulation in CS_2, the following experiments have been conducted. The clear and regular modulation spectra of self-phase modulation on both Stokes and anti-Stokes sides, the same as that in Refs. [14,22–23], are observed, when the experimental condition is the same as that of curve *A* in Fig. 9, except for inserting a line-shape filter between the polychromator and streak camera to absorb the pump line. When the pump density increases, the

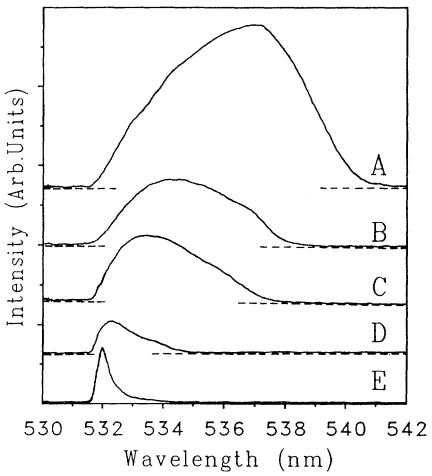

FIG. 10. Spectra of SDLS in a CS_2 bulk liquid cell excited by a frequency-doubled mode-locked Nd:YAG laser of 160 GW/cm^2 average power density: curve *A*, the peak of the pump pulse; curve *B*, the rise time of the pump pulse; curve *C*, the fall time of the pump pulse; curve *D*, the start of the pump pulse; curve *E*, the tail of the pump pulse.

spectra of SDLS broaden linearly proportional to the pump density and is only on the Stokes side; while slight spectral broadening of self-phase modulation with the increase of pump density is on both Stokes and anti-Stokes sides. Next, when the average pump-power density is higher than 30 GW/cm^2, the intensity of SDLS increases with pump density, while the intensity of self-phase modulation decreases with pump density. At 160 GW/cm^2 average pump-power density, the self-phase modulation is difficult to observe, and very weak stimulated Raman scattering also only appears at the tail of the pump pulse. These experimental results imply that self-phase modulation and stimulated Raman scattering can compete with SDLS at lower pump density but cannot compete at high-pump density, and demonstrate that SDLS due to dipole interaction has a higher pump-power-density dependence than stimulated Raman scattering and self-phase modulation.

The narrow broadening of curve *A* in Fig. 9 and the large broadening in Fig. 5 are measured at the same pump density. It demonstrates the effect of interaction length extension in waveguide.

The results in Figs. 9 and 10 also demonstrate that the frequency shift of SDLS at high pump density is proportional to the transient pump-power density. The explanations are as follows: first, the interaction between light-induced dipoles is proportional to pump-power density; second, the high-order SDLS will occur at this high-density pumping.

IV. SUMMARY AND CONCLUSIONS

SDLS, a Stokes broadened stimulated light scattering, may be greatly enhanced in a liquid-core waveguide. It consists of two primary contributions: one is related to intermolecular motion, including molecular orientation, damped intermolecular vibration, and molecular translational movement; the other results from the interaction between light-induced dipoles, the dipole-induced dipole interaction, and the collision-induced component. SDLS due to intermolecular motion dominates at the rise time of the pump pulse. Its threshold, which depends on intermolecular motion, is pump-pulse duration dependent. At low-density picosecond and nanosecond pulse laser pumping, only SDLS due to intermolecular motion dominates at the rise time of the pump pulse. At high pump density, SDLS due to dipole interactions appears around the peak of the pump pulse. The experimental results demonstrate that SDLS due to the interaction of dipoles is highly pump-power-density dependent. Especially, when the average power density of the picosecond pulse-pump laser is larger than 20 GW/cm^2, SDLS due to the interaction between light-induced dipoles, which does not appear in spontaneous dynamic light scattering, occurs; and the frequency shift is proportional to the transient pump-power density. At high pump density, the frequency shift of SDLS covers hundreds of wave numbers in bulk CS_2 liquid and 5000 cm^{-1} in a liquid-core waveguide, and SDLS dominates not only at the rise time but also around the peak of the pump pulse, while very weak stimulated Raman scattering only appears at the tail of the pump pulse.

[1] R. Pecora, *Dynamic Light Scattering* (Plenum, New York, 1985).
[2] B. J. Berne and R. Pecora, *Dynamic Light Scattering* (Wiley-Interscience, New York, 1976).
[3] D. R. Bauer, J. I. Brauman, and R. Pecora, Ann. Rev. Phys. Chem. **27**, 443 (1976).
[4] D. Kivelson and P. A. Madden, Ann. Rev. Phys. Chem. **31**, 523 (1980).
[5] T. I. Cox and P. A. Madden, Mol. Phys. **39**, 1487 (1980); **43**, 287 (1981).
[6] P. A. Madden and D. J. Tildesley, Mol. Phys. **55**, 969 (1985).
[7] P. A. Madden, Mol. Phys. **36**, 365 (1978).
[8] S. L. Shapiro and H. P. Broida, Phys. Rev. **154**, 129 (1967).
[9] M. A. F. Scarparo, J. H. Lee, and J. J. Song, Opt. Lett. **6**, 193 (1981).
[10] B. Hegemann and J. Jonas, J. Chem. Phys. **82**, 2845 (1985).
[11] N. Bloembergen and P. Lallemand, Phys. Rev. Lett. **16**, 81 (1966).
[12] R. Y. Chiao, P. L. Keeley, and E. Garmire, Phys. Rev. Lett. **17**, 1158 (1966).
[13] C. W. Cho, N. D. Foltz, D. H. Rank, and T. A. Wiggins, Phys. Rev. Lett. **18**, 107 (1967).
[14] Y. R. Shen, *The Principles of Nonlinear Optics* (Wiley, New York, 1984), pp. 195–199 and 324–329.
[15] J. Y. Zhou, H. Z. Wang, and Z. X. Yu, Appl. Phys. Lett. **57**, 643 (1990).
[16] J. Y. Zhou, H. Z. Wang, X. G. Huang, Z. G. Cai, and Z. X. Yu, Opt. Lett. **16**, 1865 (1991).
[17] J. Y. Zhou, H. Z. Wang, and Z. X. Yu, J. Mod. Opt. **38**,

1015 (1991).
[18] G. S. He and P. N. Prasad, Opt. Commun. **73**, 161 (1989).
[19] G. S. He and P. N. Prasad, Phys. Rev. A **41**, 2687 (1990).
[20] D. Wang and G. Rivoire, J. Chem. Phys. **98**, 9279 (1993).
[21] Y. X. Yan and K. A. Nelson, J. Chem. Phys. **87**, 6257 (1987).
[22] F. Shimizu, Phys. Rev. Lett. **19**, 1097 (1967).
[23] T. K. Gustafson, J. P. Taran, H. A. Haus, J. R. Lifsitz, and P. L. Kelley, Phys. Rev. **177**, 306 (1969).